Springer

Journal of
Mechanical
Science and
Technology

Journal of Mechanical Science and Technology 23 (2009) 2350~2356

www.springerlink.com/content/1738-494x
DOI 10.1007/s12206-009-0629-4

Experiments on cavitation instability of a two-bladed turbopump inducer †

Kyoung-Hoon Lee[1,*], Joo-Hyung Yoo[2] and Shin-Hyoung Kang[3]

[1]*Principal Research Engineer, Hyundai Rotem Company, Sam Dong, Uiwang-Shi, Kyunggi-Do, Republic of Korea, 437-718*
[2]*Graduate Student, School of Mechanical and Aerospace Engineering, Seoul National University, Sin-Lim Dong, Gwan-Ak Gu, Seoul, Republic of Korea, 151-742*
[3]*Professor, Department of Mechanical and Aerospace Engineering, Seoul National University, Sin-Lim Dong, Gwan-Ak Gu, Seoul, Republic of Korea, 151-742*

(Manuscript Received September 7, 2007; Revised June 1, 2008; Accepted May 25, 2009)

Abstract

The turbopump is a pressurizing system that supplies liquid propellants to the combustion chamber of a rocket engine at high pressure. As an integral component of a high-speed pumping system, the inducer used in a turbopump is forward-attached to an impeller to improve suction performance. This paper describes an experimental investigation on the flow instabilities of a two-bladed axial inducer due to cavitation. Cavitation development and its instabilities were analyzed. Asymmetric cavitation and cavitation surge were observed, and characterized by measuring the inlet pressure fluctuation for various cavitation numbers and flow coefficients. As flow coefficient decreases, the increased intensity of asymmetric cavitation was observed with an increased inception number of asymmetric cavitation. The frequency of the detected cavitation surge in the 4-10Hz range varied depending on the cavitation number. The instantaneous transition to cavitation surge appeared at the end of asymmetric cavitation as the cavitation number decreased. However, a further decrease in cavitation number resulted in the stable operation of the inducer with low values of pressure fluctuation. Finally, an intensive cavitation surge appeared after a significant amount of head loss.

Keywords: Turbopump; Inducer; Cavitation; Instability

1. Introduction

Cavitation instability is one of the most important issues in the development of reliable turbopump inducers for rocket engines. It has various modes, such as cavitation surges and rotating cavitation, as well as their high-order modes. These instabilities can induce an oscillating flow rate and pressure that can threaten the structural integrity of the pump, or its inlet and discharge ducts. Unlike a rotating stall and surge, cavitation instabilities can occur even at the design point, making the problem more serious. During the development stage of high-performance turbopump, a super-synchronous shaft vibration was observed, which was attributed to the rotating cavitation [1, 2]. The major feature of rotating cavitation is that the cavitated region rotates faster than the impeller. In order to design a more reliable turbopump inducer, it is important to understand these cavitation instabilities and suppress them, if necessary.

Another feature of the cavitation instabilities often observed in a three-bladed inducer is the asymmetric cavitation with uneven cavities on each blade [2]. It causes a large amplitude synchronous shaft vibration, because the mean blade stresses on the blades near the leading edge are significantly different owing to the asymmetry of the cavities on each blade. However, the fluctuation of the stresses on each blade remains

† This paper was recommended for publication in revised form by Associate Editor Sungbae Lee

*Corresponding author. Tel.: +82 31 596 9515, Fax.: +82 31 596 9747
E-mail address: marklee@hyundai-rotem.co.kr

© KSME & Springer 2009

low since the relative flow in the rotating frame is steady. This asymmetric cavitation phenomenon was also observed during the firing test of the LE-7A engine for the H-IIA rocket [3]. While many researchers have reported various modes of cavitation instabilities, including higher-order rotating cavitation [4], a complete classification of the various types of unsteady flow arising from cavitation has yet to be constructed.

The objective of the present study is to identify the types of cavitation instabilities of the two-bladed test inducer, and investigate their characteristics for various flow rates and inlet pressure conditions. In this study, asymmetric cavitation was observed, and its occurrence range and intensity were characterized for the variations in flow rate. The cavitation surge by extensive cavitation development was studied by frequency analysis of the inlet pressure fluctuation and flow visualization.

2. Experimental set-up and method

The test facility used in the present study is shown in Fig. 1, where the apparatus has a closed loop tunnel, and the inducer is driven by an inverter-controlled electric motor. The flow rate is controlled by the gate valve installed near the top of the tank and measured by an electro-magnetic flow meter. Tap water is used, but its impurities are filtered out and resolved gas is eliminated. The inlet pressure is controlled by the vacuum pump connected to the top of the tank. The rotational speed of the test inducer ranges from 1,800 to 3,600 rpm, and the variation in flow coefficients ranges from $0.6\,\phi_d$ to $1.1\,\phi_d$.

Details of the test section and the locations of pressure measurement on the casing wall are shown in Fig. 2. The casing wall has pressure taps used to measure the axial distribution of static pressure, and is made of transparent acryl so that the cavity on the blade can be observed with a stroboscope. The inner diameter of the casing is gradually reduced along the axial direction. To analyze the unsteady cavitation phenomenon, inlet pressure fluctuation is obtained at a sampling rate of 2.4 kHz for 30 seconds. Two pressure sensors (PGM-5KC, Kyowa) at a 90° angular distance are flush-mounted on the casing wall at 26 mm upstream of the blade tip at the inducer inlet

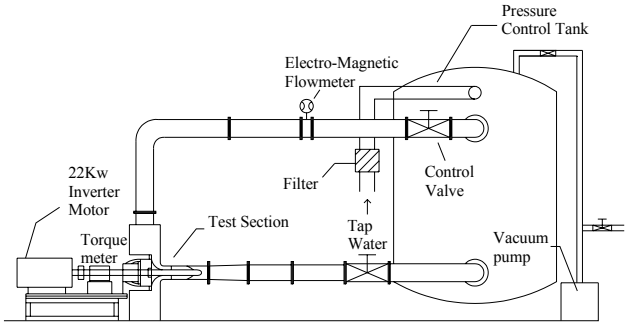

Fig. 1. Schematic of the test facility.

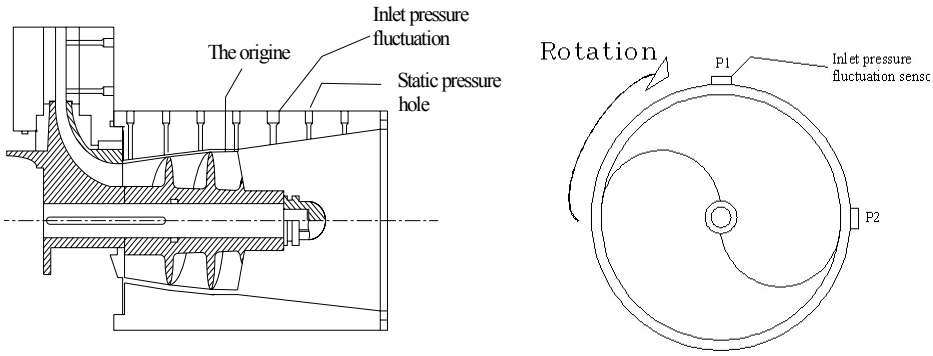

Fig. 2. Schematic of the test section.

Table 1. Specification of test inducer.

Parameters	Inducer	
	Tip	Hub
Blade inlet angle (^{0})	8.7	17.9
Blade outlet angle (^{0})	21.3	31
Inlet blade diameter (mm)	108	48
Outlet blade diameter (mm)	90	54
Inlet tip clearance (mm)	1.0	
Solidity at mean diameter	2.4	
Number of blades	2	
Design flow coefficient	0.078	
Tip incidence angle (deg.)	4	

(a) Test inducer

(b) Test rig

Fig. 3. Photographs of (a) test inducer and (b) test rig.

Fig. 3 shows the test inducer. It has an increasing hub diameter with decreasing shroud diameter along the axial direction. The specifications of the inducer are shown in Table 1. The inducer has two blades with a swept-back leading edge, with blade angles at the inlet and outlet tips at 8.7˚and 21.3˚, respectively. Radial tip clearance is 1.0 mm. The solidity at mid-span has a value of 2.4. The design flow coefficient is 0.078.

Flow unsteadiness is investigated by Fourier analysis of signals coming from the pressure transducers installed in the inducer casing. The nature of the axial surge or rotating cavitation and the number of rotating cells are analyzed by cross-correlation between the two pressure signals that are obtained at different angular positions. For an axial phenomenon, the phase of the cross-correlation between the two pressure signals is equal to 0˚. For a rotating phenomenon, the ratio of the phase of the cross-correlation (φ) to the angular separation between the transducers ($\Delta\theta$) has to be an integer that is equal to the number of rotating cells (n_{cell}).

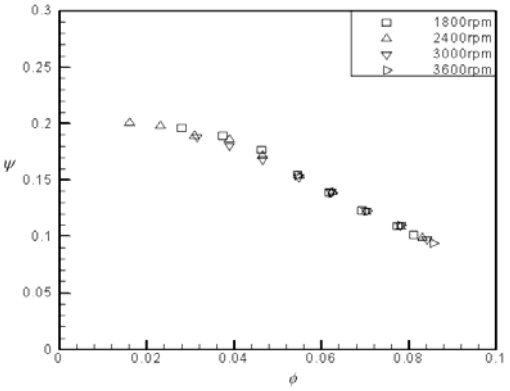

Fig. 4. Variations in head coefficient with flow coefficient.

$$n_{cell} = \varphi / \Delta\theta \tag{1}$$

If f_d is the detected frequency of the pressure oscillation, the real frequency of the oscillation (f_r) is given by

$$f_r = f_d \cdot \Delta\theta / \varphi = f_d / n_{cell} \tag{2}$$

3. Test results and discussion

Fig. 4 shows non-dimensional total-static head performance variations without cavitation for four different speeds. They show good similarity with the 1,800-3,600 rpm range. Fig. 5 presents the efficiency variations, with the maximum efficiency achieved near the design flow coefficient (ϕ_d =0.078). Fig. 6 shows the cavitation performance of the test inducer for flow coefficients of $0.6\,\phi_d$, $0.8\,\phi_d$, $1.0\,\phi_d$, and $1.1\,\phi_d$. As the cavitation number decreased, the pressure rise performance likewise decreased owing to cavitation, but asymmetric cavitation and cavitation surge appears. The asymmetric cavitation, which has the same frequency as the rotational speed of the inducer, is observed in all the tested ranges of the flow coefficient. Its inception begins just after the initiation of the head drop caused by cavitation. The onset point and occurrence region are similar to the result observed in [3].

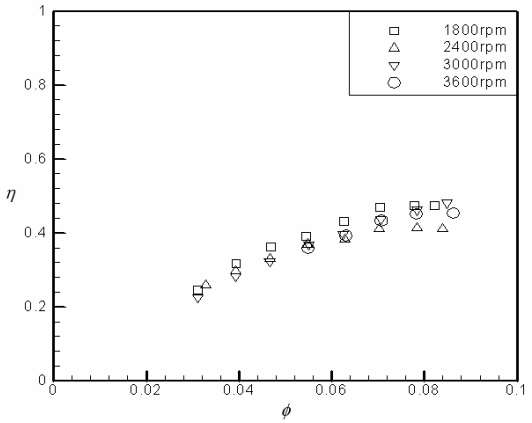

Fig. 5. Variations in efficiency with flow coefficient.

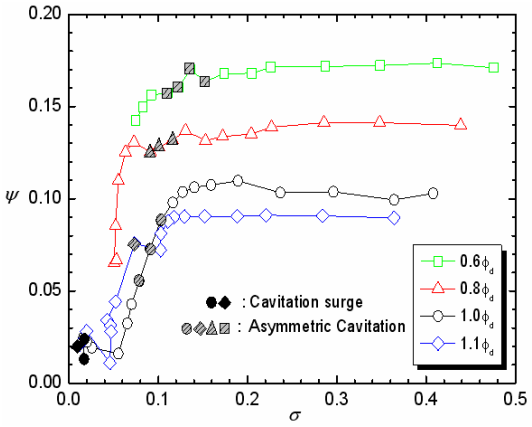

Fig. 6. Variations in performances for different values of cavitation number and flow coefficient at 3600 rpm.

It is known that cavitation surge occurs more readily when the inducer is more heavily loaded, in other words, at lower flow coefficients when backflow occurs [5]. However, in this study, cavitation surge is more readily observed after the substantial head breakdown at flow coefficients of $1.0\phi_d$ and $1.1\phi_d$ rather than at the expected lower flow coefficients. Fig. 7 presents the cavitation numbers for 5%, 15%, and 30% head drops. The gap in cavitation numbers between breakdown point and the beginning of head decrease is larger at low flow coefficients ($0.6\phi_d$, $0.8\phi_d$) compared to the design flow coefficients (ϕ_d). Fig. 8(a), (b), (c), and (d) show the cascade plot of the spectrum of inlet pressure fluctuations for various cavitation numbers. The flow coefficients are 0.6, 0.8, 1.0, and 1,1 of $\phi_d (= 0.078)$. The rotational speed is

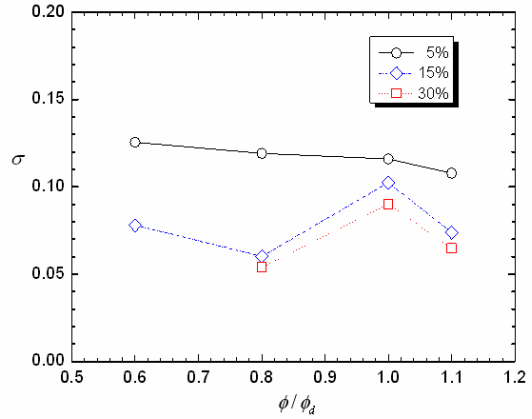

Fig. 7. Variations in cavitation numbers for 5%, 15%, and 30% head coefficient losses at 3600 rpm.

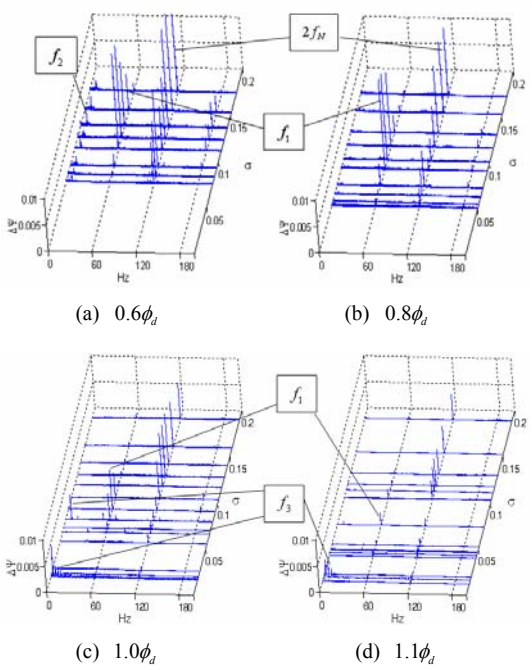

(a) $0.6\phi_d$ (b) $0.8\phi_d$

(c) $1.0\phi_d$ (d) $1.1\phi_d$

Fig. 8. Spectral analysis of inlet pressure for different values of flow coefficient at 3600 rpm.

3,600 rpm, so the blade passing frequency is 120Hz($2 f_N$). In the case of asymmetric cavitation with a component of 60Hz($f/f_N = 1.0$), its pressure fluctuation coefficients are large at the low flow coefficient, and the inception number of the asymmetric cavitation also increases as flow coefficient decreases.

The component denoted by " f_2 " is observed at flow coefficient $0.6\phi_d$. This component is caused by the rotating instability with a single rotating cell, as

Table 2. Flow instability detected in the test inducer.

	Type of instability	Frequency
f_1	Asymmetric cavitation	f_N
f_2	Rotating stall	0.15 f_N
f_3	Cavitation surge	4-10Hz

confirmed by the analysis of the phase difference of the cross-correlation, and occurs also without cavitation. The rotating stall is expected to be induced because of the high incidence angle and inlet backflow, resulting from its disappearance at high flow coefficient. In the cases of ϕ_d and 1.1 ϕ_d, a component of f_3 observed near the value of σ=0.015 is identified as the axial instability with 0° phase difference of the cross-spectrum between the two inlet pressure signals, implying a cavitation surge phenomenon. The frequency range of the cavitation surge is 4-10 Hz. The frequency slightly increases with increasing cavitation number. Table 2 summarizes the types of cavitation instabilities that were observed during the test. Figs. 9(a)-(e) show the wave forms of pressure signals, and the results of Fourier analysis for various cavitation numbers. Similarly, Fig. 9(a) shows the inlet pressure fluctuation without cavitation at σ=0.4079, wherein the blade passing frequency (120Hz=2 f_N) is only detected in its fast fourier transform (FFT). Incidentally, also in Fig. 9(b), asymmetric cavitation becomes dominant at σ=0.0908, and its fluctuation magnitude becomes larger than the blade passing frequency. Surge mode (9Hz) and weak components of rotating cavitation (0.95 f_N, 1.15 f_N) are observed at σ=0.079 (Fig. 9(c)), the cavitation number wherein asymmetric cavitation weakens. With the low magnitude of pressure fluctuation, a further decrease of the cavitation number leads to the stable operation of the inducer, as seen in Fig. 9(d). An extensive cavitation surge, with peak pressure fluctuation at 4 Hz, follows a cavitation breakdown (Fig. 9(e)). The phase of the cross-correlation at the frequency of the cavitation surge is clearly at 0°, thus manifesting axial instability.

Fig. 10 shows the progress of the cavitating region for various cavitation numbers at the low flow coefficient (0.8 ϕ_d). As inlet pressure decreases, the inception of cavitation occurs in the tip vortex, which is generated by the corner wherein the leading edge meets the tip (σ=0.438). As cavitation develops, cavitation cavities fill the inlet of the inducer. However, there is no significant cavity infiltration

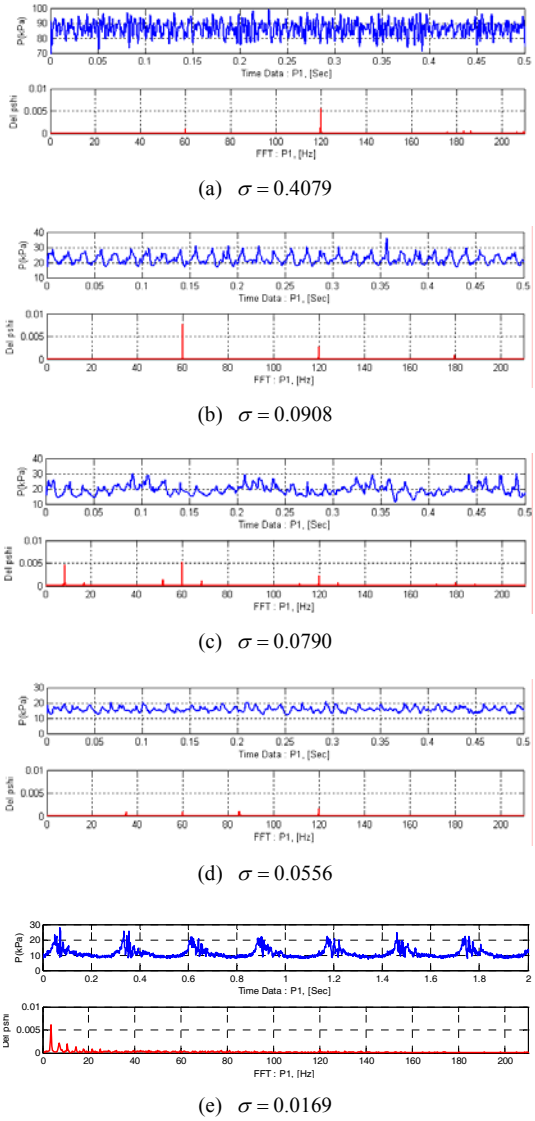

(a) $\sigma = 0.4079$

(b) $\sigma = 0.0908$

(c) $\sigma = 0.0790$

(d) $\sigma = 0.0556$

(e) $\sigma = 0.0169$

Fig. 9. Pressure and spectrum of inlet pressure fluctuation for different cavitation numbers at ϕ_d and 3600 rpm.

into the blade channel at this stage (σ=0.136). The occurrence of backflow, which is clearly evident at this stage, makes the cavitation bubbles that are generated from the tip leading edge to move upstream and stay in the backflow zone. The further decrease of the inlet pressure leads to a substantial head drop. The infiltration of the cavitating region into the blade passage is clearly observed at this stage (σ=0.091), and "backflow cavitation," referring to the cavitating bubbles in the annular region of backflow upstream to the inlet, becomes obvious. A further decrease of the inlet pressure leads to an abrupt cavitation breakdown.

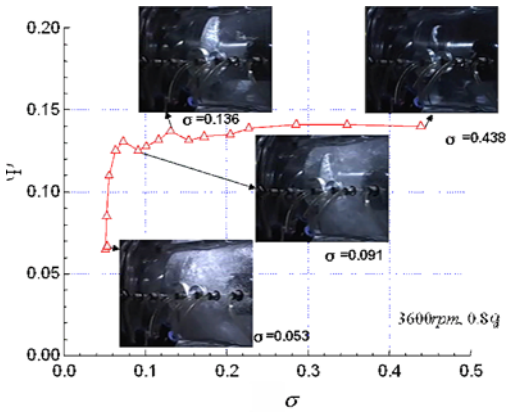

Fig. 10. Development of cavitation for $0.8\phi_d$ and 3600 rpm.

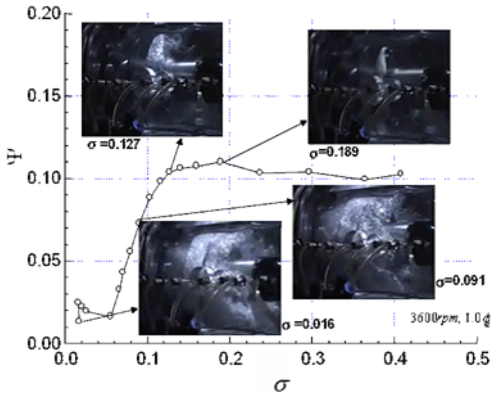

Fig. 11. Development of cavitation for ϕ_d and 3600 rpm.

Fig. 11 shows the design flow coefficient (ϕ_d). There is a moderate backflow even at the design flow coefficient. The cavities develop similar to the case shown in Fig. 10. When cavitation has extended sufficiently to provide complete saturation of the blade channel, the head coefficient begins to reduce, and breakdown conditions are achieved (σ =0.055). An extensive cavitation surge below the cavitation number (σ =0.055) is observed with discrete breeding noise, and Fig. 12 shows the details of the cavitation surge for a very low cavitation number (σ =0.0169). Flow oscillation with large amplitude and low frequency in the axial direction results in dramatic changes in the shape of the cavities. The photographs of the cavities under asymmetric cavitation are shown in Fig. 13. The blade with a short cavity (Fig. 13(a)) and long cavity (Fig. 13(b)) are observed. This result means that there are different-sized cavities on the two blades.

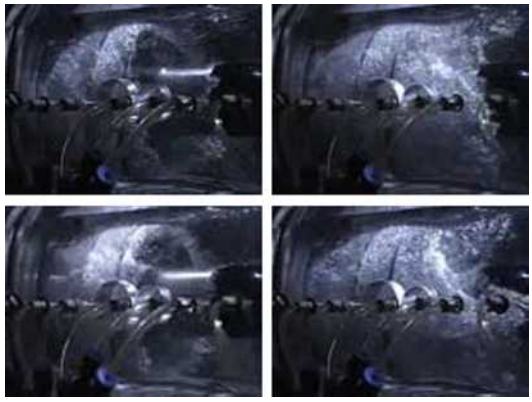

Fig. 12. Photographs of cavitation surge for $\sigma = 0.0169$, ϕ_d and 3600 rpm.

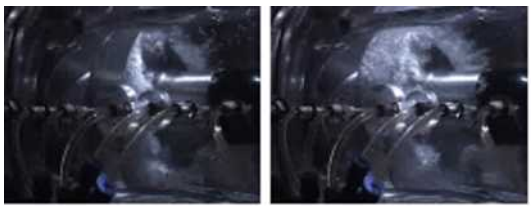

(a) Shorter cavity (b) Longer cavity

Fig. 13. Photographs of asymmetric cavitation for $\sigma = 0.091$, ϕ_d and 3600 rpm.

4. Conclusions

With the two-bladed inducer, several flow instabilities were observed in the experiment. The following characteristics of these instabilities were found by measurements of the inlet pressure fluctuations.

(1) Asymmetric cavitation with steady unequal cavities on each blade was observed in the spectra of inlet pressure fluctuations and flow visualization. The intensity of asymmetric cavitation increases with the decreased flow coefficient and the inception number of asymmetric cavitation also increases as flow coefficient decreases.

(2) A cavitation surge, an axial instability confirmed by analyzing the cross-correlation phase and flow visualization, was observed. The frequency range of this mode was 4-10 Hz, depending on the cavitation number.

(3) The instantaneous transition to cavitation surge appeared at the end of the asymmetric cavitation with decreasing cavitation number. A further decrease of the cavitation number resulted in stable operation with low values of pressure fluctuation. Finally, an intensive cavitation surge appeared af-

ter a significant amount of head drop.

Nomenclature

D : Inducer diameter
f : Frequency
f_d : Detected frequency
f_r : Real frequency
f_N : Shaft rotational frequency
u : Axial velocity
ρ : Density
U_{tip} : Peripheral speed of inducer inlet $(=\pi D_1 f_N)$
σ : Cavitation number $(=(p_1 - p_v)/(0.5\rho U_{tip}^2))$
ϕ : Flow coefficient $(=u_1/U_{tip})$
$\Delta\Psi$: Head fluctuation coefficient $(=\Delta p/(\rho U_{tip}^2))$
Ψ : Head coefficient $(=(p_{2s} - p_{1t})/(\rho U_{tip}^2))$
$\Delta\theta$: Angular separation between pressure transducers
n : The number of rotating cells
φ : Phase difference of cross-correlation

Subscripts

d : Design point
1 : Inducer inlet
2 : Inducer outlet
t : Total
s : Static

Reference

[1] K. Kamijo, M. Yoshida and Y. Tsujimoto, Hydraulic and Mechanical Performance of LE-7 LOX Pump Inducer, *AIAA Journal of Propulsion and Power*, *9, 6,* (1993) 819-826.
[2] Y. Tsujimoto and Y. Yoshida, Observation of Oscillating Cavitation of an Inducer, *Journal of Fluids Engineering, 119,* (1997) 775-781.
[3] A. Fujii and S. Azuma, Unsteady Behavior of Asymmeric Cavitation in a 3-Bladed Inducer, *5th International Symposium on Cavitation(Cav2003),* Osaka, Japan, (2003).
[4] A. Fujii and S. Azuma, Higher Order Rotating Cavitation in an Inducer, *International Journal of Rotating Machinery*, 10 (4) (2004) 241-251.
[5] C. E. Brennen, Hydrodynamics of Pumps, Concepts ETI, Inc Oxford University Press, (1994).
[6] Y. Tsujimoto and H. Horiguchi, Backflow from Inducer and its Dynamics, *ASME Fluids Engineering Division Summer Meeting and Exhibition, FEDSM2005-77381*. (2005).

Kyoung-Hoon Lee received his M.S. degree in Mechanical engineering from Seoul National University in 1993. He has focused on turbo-machinery design including turbo-pump system in space rocket propulsion, and currently works as a principal research engineer in Hyundai Rotem Company, Korea.

Joo-Hyung Yoo received his M.S. degree in Mechanical engineering from Seoul National University in 2006 and currently involves in the defense industry as a design engineer in Hanwha Corporation, Korea.

Shin-Hyoung Kang received his B.S. degree in Mechanical Engineering from Seoul National University, in 1973. He then received his M.S. in Korea Advance Institute of Korea in 1975 and Ph.D. degrees from University of Iowa in 1978, respectively. Dr. Kang is currently a Professor at the School of Mechanical Engineering at Seoul National University in Seoul, Korea. He served as President of KFMA, President of SAREK, and President of KSME. Dr. Kang's main research interests is fluids machinery .